Supplementary Materials for "Analysis of Cardiac Mitochondrial Na^+/Ca^{2+} Exchanger Kinetics with a Biophysical Model of Mitochondrial Ca^{2+} Handing Suggests a 3:1 Stoichiometry"

Ranjan K. Dash and Daniel A. Beard

Biotechnology and Bioengineering Center and Department of Physiology, Medical College of Wisconsin, Milwaukee, WI-53226

Address for correspondence: Daniel A. Beard, Biotechnology and Bioengineering Center, Medical College of Wisconsin, 8701 Watertown Plank Road, Milwaukee, WI 53226, Phone: (414) 456-5752, Fax: (414) 955-6317, Email: dbeard@mcw.edu

Computational Model of Mitochondrial Oxidative Phosphorylation

This appendix presents a simplified version of our computational model of mitochondrial respiratory system and oxidative phosphorylation (Beard, 2005) (also see Beard, 2006; Huang *et al.*, 2007; Wu *et al.*, 2007a; Wu *et al.*, 2007b) which constitute a key component of the present integrated model of mitochondrial bioenergetics and Ca^{2+} handling. The kinetics of Na^+-Ca^{2+} transport system are coupled to the kinetics of electron transport system and oxidative phosphorylation via the inner mitochondrial membrane (IMM) potential $\Delta\Psi$ and trans-IMM pH gradient (or proton motive force ΔG_H). The basic components of the original model include reactions at complexes I, III, IV and V, substrate transporters ANT (adenine nucleotide translocase) and PHT (phosphate-hydrogen cotransporter), and cation fluxes across the IMM, including the fluxes via the KHE (K^+/H^+ exchanger) and passive H^+ and K^+ permeations ("leaks") (Figure 1). The simplifications include deletion of the adenylate kinase reaction in the intermembrane space which has a very little role in the regulation mitochondrial bioenergetics in isolated mitochondria. In addition, the bindings of magnesium ions (Mg^{2+}) to the adenine nucleotides (ATP and ADP) are assumed fast so that the reactions can be considered at near equilibrium at all time. These simplifications reduce the number of differential equations to solve governing the biochemical processes of energy metabolism in mitochondria. For clarity, the simplified governing model equations are presented below and the associated model parameter values are presented in Table S1.

Mitochondrial Transport and Reaction Fluxes:

Dehydrogenase $\quad NAD^+ \rightleftarrows NADH + H^+$

$$J_{DH} = X_{DH}\left(\frac{1+[Pi]_x/k_{Pi,1}}{1+[Pi]_x/k_{Pi,2}}\right)\left(r_{DH}\,[NAD^+]_x - [NADH]_x\right)$$

The model do not account for the kinetics of the TCA cycle and other NADH-producing reactions (Beard, 2005, 2006; Wu *et al.*, 2007a). Instead, the rate of NADH production from NAD^+ is modeled using a phosphate-dependent phenomenological dehydrogenase flux expression.

Complex I $\mathrm{H^+ + NADH + UQ \rightleftarrows NAD^+ + UQH_2 + 4\,\Delta H^+}$

$$J_{C1} = X_{C1}\left(\begin{array}{c}\exp\left(-\left(\Delta G_{o,C1} + 4\Delta G_H - RT\ln([H^+]_x/10^{-7})\right)/RT\right)\\ \times[NADH]_x[UQ] - [NAD^+]_x[UQH_2]\end{array}\right)$$

where $\Delta G_H = F\Delta\Psi + RT\ln([H^+]_e/[H^+]_x)$ is the proton motive force, or the change in Gibb's free energy associated with the pumping of protons from the matrix side to the extra-matrix side of the IMM. A total of 4 protons are pumped each time this reaction proceeds.

Complex III $\mathrm{UQH_2 + 2\ cyt\text{-}c(ox)^{3+} \rightleftarrows UQ + 2\ cyt\text{-}c(red)^{2+} + 2\ H^+ + 4\ \Delta H^+}$

$$J_{C3} = X_{C3}\left(\frac{1+[Pi]_x/k_{Pi,3}}{1+[Pi]_x/k_{Pi,4}}\right)\left(\begin{array}{c}\exp\left(-\left(\Delta G_{o,C3} + 4\Delta G_H + 2RT\ln([H^+]_x/10^{-7}) - 2F\Delta\Psi\right)/2RT\right)\\ \times[\text{cyt-c(ox)}^{3+}][UQH_2]^{1/2} - [\text{cyt-c(red)}^{2+}][UQ]^{1/2}\end{array}\right)$$

The model accounts for a phosphate-dependent control of the complex III reaction. A total of 4 protons are pumped from the matrix side to the extra-matrix side of the IMM each time this reaction proceeds.

Complex IV $\mathrm{2\ H^+ + 2\ cyt\text{-}c(red)^{2+} + 0.5\ O_2 \rightleftarrows 2\ cyt\text{-}c(ox)^{3+} + H_2O + 2\ \Delta H^+}$

$$J_{C4} = X_{C4}\left(\frac{[O_2]}{k_{O_2}+[O_2]}\right)\left(\frac{[\text{cyt-c(red)}^{2+}]}{\text{cyt-c}_{tot}}\right)\left(\begin{array}{c}\exp\left(-\left(\Delta G_{o,C4} + 2\Delta G_H - 2RT\ln([H^+]_x/10^{-7})\right)/2RT\right)\\ \times[\text{cyt-c(red)}^{2+}][O_2]^{1/4} - e^{+F\Delta\Psi/RT}[\text{cyt-c(ox)}^{3+}]\end{array}\right)$$

A total of 2 protons are pumped from the matrix side to the extra-matrix side of the IMM each time this reaction proceeds (oxygen consumption).

Complex V (F_1F_0-ATPase) $\mathrm{H^+ + ADP + Pi + }n_{F1F0}\,\Delta H^+ \rightleftarrows \mathrm{ATP}$

$$J_{F1F0} = X_{F1F0}\left(\begin{array}{c}\exp\left(-\left(\Delta G_{o,F1F0} - n_{F1F0}\Delta G_H - RT\ln([H^+]_x/10^{-7})\right)/RT\right)\\ \times\left(K_{MgADP}/K_{MgATP}\right)[mADP]_x[Pi]_x - (1\ M)[mATP]_x\end{array}\right)$$

A total of n_{F1F0} (= 3) protons enter the matrix through the proton channel of F_1F_0-ATPase each time this reaction proceeds (ATP synthesis).

Magnesium Binding $\mathrm{Mg^{2+} + fATP \rightleftarrows mATP;}\quad \mathrm{Mg^{2+} + fADP \rightleftarrows mADP}$

$$[mATP] = \frac{[ATP][Mg^{2+}]}{K_{MgATP}+[Mg^{2+}]} \quad \text{and} \quad [mADP] = \frac{[ADP][Mg^{2+}]}{K_{MgADP}+[Mg^{2+}]}$$

$$[fATP] = \frac{K_{MgATP}[ATP]}{K_{MgATP}+[Mg^{2+}]} \quad \text{and} \quad [fADP] = \frac{K_{MgADP}[ADP]}{K_{MgADP}+[Mg^{2+}]}$$

$$[Mg^{2+}]_{tot} = [Mg^{2+}] + [mATP] + [mADP]$$

These relationships are based on equilibrium binding of Mg^{2+} with fATP and fADP. So given [ATP], [ADP] and $[Mg^{2+}]_{tot}$ (total concentrations) in a compartment (x, i or e), the $[Mg^{2+}]$,

[fATP], [fADP] (free concentrations), and [mATP] and [mADP] (bound concentrations) can be obtained from the above equilibrium binding relationships. In fact, the problem reduces to solving the following cubic polynomial for the free Mg^{2+} concentration, $[Mg^{2+}]$:

$$A_0 + A_1[Mg^{2+}] + A_2[Mg^{2+}]^2 + A_3[Mg^{2+}]^3 = 0$$

where

$$A_0 = -[Mg^{2+}]_{tot} K_{MgATP} K_{MgADP}$$

$$A_1 = K_{MgADP}[ATP] + K_{MgATP}[ADP] - [Mg^{2+}]_{tot}(K_{MgATP} + K_{MgADP}) + K_{MgATP}K_{MgADP}$$

$$A_2 = [ATP] + [ADP] - [Mg^{2+}]_{tot} + K_{MgATP} + K_{MgADP}$$

$$A_3 = 1$$

Once the free $[Mg^{2+}]$ is obtained from the above cubic polynomial, [fATP], [fADP], [mATP] and [mADP] can be obtained from the associated equilibrium binding relationships.

Adenine Nucleotide Translocase (ANT)

$$J_{ANT} = X_{ANT}\left(\frac{[fADP]_i}{k_{ADP} + [fADP]_i}\right)\left(\frac{[fADP]_i}{[fADP]_i + [fATP]_i e^{-0.35F\Delta\Psi/RT}} - \frac{[fADP]_x}{[fADP]_x + [fATP]_x e^{+0.65F\Delta\Psi/RT}}\right)$$

The exchange of ATP for ADP via the ANT is electrogenic, so the flux is dependent on the IMM potential $\Delta\Psi$. In addition, the exchange is regulated (activated) by the extra-matrix free ADP concentration.

Phosphate-Hydrogen Cotransporter (PHT)

$$J_{PHT} = X_{PHT}\left(\frac{[H_2PO_4^-]_x[H^+]_x - [H_2PO_4^-]_i[H^+]_i}{[H_2PO_4^-]_i + k_{PHT}}\right)$$

where $[H_2PO_4^-]_i = [H^+]_i[Pi]_i / \left([H^+]_i + k_{dH}\right)$, $[H_2PO_4^-]_x = [H^+]_x[Pi]_x / \left([H^+]_x + k_{dH}\right)$ and $[H^+]_i = [H^+]_e$.

Pottasium-Hydrogen Exchanger (KHE)

$$J_{KHE} = X_{KHE}\left([K^+]_i[H^+]_x - [K^+]_x[H^+]_i\right); \quad [K^+]_i = [K^+]_e \text{ and } [H^+]_i = [H^+]_e$$

Passive Proton Permeation (Leak)

$$J_{Hleak} = X_{Hleak}\Delta\Psi\left(\frac{[H^+]_i \exp(+F\Delta\Psi/RT) - [H^+]_x}{\exp(+F\Delta\Psi/RT) - 1}\right); \quad [H^+]_i = [H^+]_e$$

Passive Pottasium Permeation (Leak)

$$J_{Kleak} = X_{Kleak}\Delta\Psi\left(\frac{[K^+]_i \exp(+F\Delta\Psi/RT) - [K^+]_x}{\exp(+F\Delta\Psi/RT) - 1}\right); \quad [K^+]_i = [K^+]_e$$

Passive Substrate Transport Fluxes

$$J_{\mathrm{ATPt}} = \gamma p_{\mathrm{A}} \left([\mathrm{ATP}]_{\mathrm{e}} - [\mathrm{ATP}]_{\mathrm{i}} \right)$$
$$J_{\mathrm{ADPt}} = \gamma p_{\mathrm{A}} \left([\mathrm{ADP}]_{\mathrm{e}} - [\mathrm{ADP}]_{\mathrm{i}} \right)$$
$$J_{\mathrm{Pit}} = \gamma p_{\mathrm{Pi}} \left([\mathrm{Pi}]_{\mathrm{e}} - [\mathrm{Pi}]_{\mathrm{i}} \right)$$

Dynamic Mass Balance Equations:

The following differential equations constitute the simplified model of mitochondrial electron transport system and oxidative phosphorylation. This model is further augmented by the differential equations for Na^+ and Ca^{2+} in the matrix and extra-matrix spaces (see the Method section).

$$d\Delta\Psi/dt = (+4J_{\mathrm{C1}} + 2J_{\mathrm{C3}} + 4J_{\mathrm{C4}} - n_{\mathrm{F1F0}}J_{\mathrm{F1F0}} - J_{\mathrm{ANT}} - J_{\mathrm{Hleak}} - J_{\mathrm{Kleak}}) / C_{\mathrm{IMM}}$$
$$d[\mathrm{H}^+]_{\mathrm{x}}/dt = [\mathrm{H}^+]_{\mathrm{x}}(+J_{\mathrm{DH}} - 5J_{\mathrm{C1}} - 2J_{\mathrm{C3}} - 4J_{\mathrm{C4}} + (n_{\mathrm{F1F0}} - 1)J_{\mathrm{F1F0}} + 2J_{\mathrm{PHT}} + J_{\mathrm{Hleak}} - J_{\mathrm{KHE}}) / (\beta_{\mathrm{H}} W_{\mathrm{x}})$$
$$d[\mathrm{K}^+]_{\mathrm{x}}/dt = \left(+J_{\mathrm{KHE}} + J_{\mathrm{Kleak}}\right)/W_{\mathrm{x}}$$
$$d[\mathrm{NADH}]_{\mathrm{x}}/dt = \left(+J_{\mathrm{DH}} - J_{\mathrm{C1}}\right)/W_{\mathrm{x}}$$
$$d[\mathrm{UQH_2}]_{\mathrm{x}}/dt = \left(+J_{\mathrm{C1}} - J_{\mathrm{C3}}\right)/W_{\mathrm{x}}$$
$$d[\text{cyt-c(red)}^{2+}]_{\mathrm{i}}/dt = \left(+2J_{\mathrm{C3}} - 2J_{\mathrm{C4}}\right)/W_{\mathrm{i}}$$
$$d[\mathrm{ATP}]_{\mathrm{x}}/dt = \left(+J_{\mathrm{F1F0}} - J_{\mathrm{ANT}}\right)/W_{\mathrm{x}}$$
$$d[\mathrm{Pi}]_{\mathrm{x}}/dt = \left(-J_{\mathrm{F1F0}} + J_{\mathrm{PHT}}\right)/W_{\mathrm{x}}$$
$$d[\mathrm{ATP}]_{\mathrm{i}}/dt = \left(+J_{\mathrm{ATPt}} + J_{\mathrm{ANT}}\right)/W_{\mathrm{i}}$$
$$d[\mathrm{ADP}]_{\mathrm{i}}/dt = \left(+J_{\mathrm{ADPt}} - J_{\mathrm{ANT}}\right)/W_{\mathrm{i}}$$
$$d[\mathrm{Pi}]_{\mathrm{i}}/dt = \left(+J_{\mathrm{Pit}} - J_{\mathrm{PHT}}\right)/W_{\mathrm{i}}$$
$$d[\mathrm{ATP}]_{\mathrm{e}}/dt = -J_{\mathrm{ATPt}}/W_{\mathrm{e}}$$
$$d[\mathrm{ADP}]_{\mathrm{e}}/dt = -J_{\mathrm{ADPt}}/W_{\mathrm{e}}$$
$$d[\mathrm{Pi}]_{\mathrm{e}}/dt = -J_{\mathrm{Pit}}/W_{\mathrm{e}}$$

The governing differential equations for $\Delta\Psi$ and $[H^+]_x$ are further modified due to the contributions from fluxes through the CU, NCE and NHE (see the Method section). The following state variables are computed from the total concentration pools based on mass conservations:

$$[\mathrm{NAD}^+]_{\mathrm{x}} = \mathrm{NAD}_{\mathrm{tot}} - [\mathrm{NADH}]_{\mathrm{x}}$$
$$[\mathrm{UQ}] = \mathrm{UQ}_{\mathrm{tot}} - [\mathrm{UQH_2}]$$
$$[\text{cyt-c(ox)}^{3+}] = \text{cyt-c}_{\mathrm{tot}} - [\text{cytC(red)}^{2+}]$$
$$[\mathrm{ADP}]_{\mathrm{x}} = \mathrm{A}_{\mathrm{tot}} - [\mathrm{ATP}]_{\mathrm{x}}$$

Table S1: Parameter values in the simplified model of mitochondrial electron transport system and oxidative phosphorylation ("mito" denotes mitochondria). Most parameter values were estimated based on the experimental data of Bose *et al.* (2003) in isolated cardiac mitochondria. For details, see the references (Beard, 2005, 2006; Huang *et al.*, 2007; Wu *et al.*, 2007a; Wu *et al.*, 2007b).

Parameter	Description	Values	Units	Reference
Physicochemical/Thermodynamic Parameters:				
RT	Gas constant times temperature	2.5775	kJ mol^{-1}	_a
F	Faraday's constant	0.096484	kJ mol^{-1} mV^{-1}	_a
$\Delta G_{o,C1}$	Standard free energy, complex I	–69.37	kJ mol^{-1}	_b
$\Delta G_{o,C3}$	Standard free energy, complex III	–32.53	kJ mol^{-1}	_b
$\Delta G_{o,C4}$	Standard free energy, complex IV	–122.94	kJ mol^{-1}	_b
$\Delta G_{o,F1F0}$	Standard free energy, F_1F_0-ATPase	36.03	kJ mol^{-1}	_b
Anatomical Parameters:				
W_x	Matrix water fraction	0.6514	(l water) (l mito)$^{-1}$	_c
W_i	IMS water fraction	0.0724	(l water) (l mito)$^{-1}$	_c
W_e	External buffer water fraction	390.0	(l water) (l mito)$^{-1}$	_d
γ	Outer membrane area per mito volume	5.99	μm^{-1}	_e
Mitochondrial Model Parameters:				
$k_{Pi,1}$	Dehydrogenase/Pi parameter	0.1553	mM	_f
$k_{Pi,2}$	Dehydrogenase/Pi parameter	0.8222	mM	_f
r_{DH}	Dehydrogenase phenomenological parameter	4.559	unitless	_f
X_{DH}	Dehydrogenase activity	0.0866	mol s^{-1} M^{-1} (l mito)$^{-1}$	_f
X_{C1}	Complex I activity	4.405×10^{3}	mol s^{-1} M^{-2} (l mito)$^{-1}$	_f
X_{C3}	Complex III activity	4.887	mol s^{-1} M$^{-3/2}$ (l mito)$^{-1}$	_f
X_{C4}	Complex IV activity	6.766×10^{-5}	mol s^{-1} M^{-1} (l mito)$^{-1}$	_f
X_{F1F0}	F_1F_0-ATPase activity	1000.0	mol s^{-1} M^{-1} (l mito)$^{-1}$	_f
X_{ANT}	ANT activity	8.123×10^{-3}	mol s^{-1} (l mito)$^{-1}$	_f
n_{F1F0}	H^+ stoichiometry for F_1F_0-ATPase	3.0	unitless	_g
X_{PHT}	Pi^-/H^+ cotransporter activity	3.850×10^{5}	mol s^{-1} M^{-1} (l mito)$^{-1}$	_f
k_{PHT}	Pi^-/H^+ cotransporter parameter	0.2542	mM	_f
X_{KHE}	K^+/H^+ antiporter activity	5.651×10^{7}	mol s^{-1} M^{-2} (l mito)$^{-1}$	_f
X_{Hleak}	Proton leak activity	200.0	mol s^{-1}M^{-1}mV^{-1}(l mito)$^{-1}$	_f
X_{Kleak}	Potassium leak activity	0.0	mol s^{-1}M^{-1}mV^{-1}(l mito)$^{-1}$	_f
$k_{Pi,3}$	Complex III/Pi parameter	0.3601	mM	_f
$k_{Pi,4}$	Complex III/Pi parameter	5.924	mM	_f
p_{Pi}	Outer mitochondrial membrane permeability to inorganic phosphate	327.0	μm sec^{-1} (l mito)$^{-1}$	_h
p_A	Outer mitochondrial membrane permeability to nucleotides	85.0	μm sec^{-1} (l mito)$^{-1}$	_i

k_{ADP}	ANT Michaelis-Menten constant	3.5×10^{-6}	M	_h
k_{O2}	Kinetic constant for complex IV	1.2×10^{-4}	M	_h
β_H	Matrix proton buffering capacity	0.0043	M	_j
C_{IMM}	Effective capacitance of IMM	6.75×10^{-6}	mol (l mito) $^{-1}$ mV^{-1}	_k
Fixed Concentrations Pools:				
NAD_{tot}	Total matrix NAD concentration	2.97	mmol (l matrix water) $^{-1}$	_h
UQ_{tot}	Total matrix ubiquinol concentration	1.35	mmol (l matrix water) $^{-1}$	_h
cyt-c_{tot}	Total IMS cytochrome-c concentration	2.70	mmol (l IMS water) $^{-1}$	_h
A_{tot}	Total matrix adenine nucleotide concentration (ATP+ADP)	10	mmol (l matrix water) $^{-1}$	_h
$[Mg^{2+}]_{tot}$	Total matrix Mg^{2+} concentration	10	mmol (l matrix water) $^{-1}$	_h
$[H^+]_e$	Buffer H^+ ion concentration	$10^{-7.2}$	mol (l buffer water) $^{-1}$	_d
$[K^+]_e$	Buffer K^+ ion concentration	180	mmol (l buffer water) $^{-1}$	_d
$[Pi]_e$	Buffer Pi concentration	2.5	mmol (l buffer water) $^{-1}$	_d
$[O_2]$	Buffer O_2 concentration	3.48×10^{-5}	M	_d
Binding Constants:				
K_{MgATP}	Mg-ATP binding constant	24×10^{-6}	M	_h
K_{MgADP}	Mg-ADP binding constant	347×10^{-6}	M	_h
k_{dH}	H^+- $H_2PO_4^-$ dissociate constant	1.778×10^{-7}	M	_l

_a Standard physicochemical/thermodynamic constants
_b Computed from the thermodynamic data tabulated in Alberty (2003)
_c Taken from Vinnakota and Bassingthwaighte (2004)
_d Experimental condition of Cox and Matlib (1993)
_e Taken from Munoz *et al.* (1999)
_f Estimations from Beard (2005; 2006) and Wu *et al.* (2007a).
_g Taken from Tomashek & Brusilow (2000)
_h Taken from Vendelin *et al.* (2000)
_i Taken from Lee *et al.* (1994)
_j Taken from Kapus *et al.* (1989)
_k Taken from Gentet *et al.* (2000)
_l Taken from Alberty (2003)

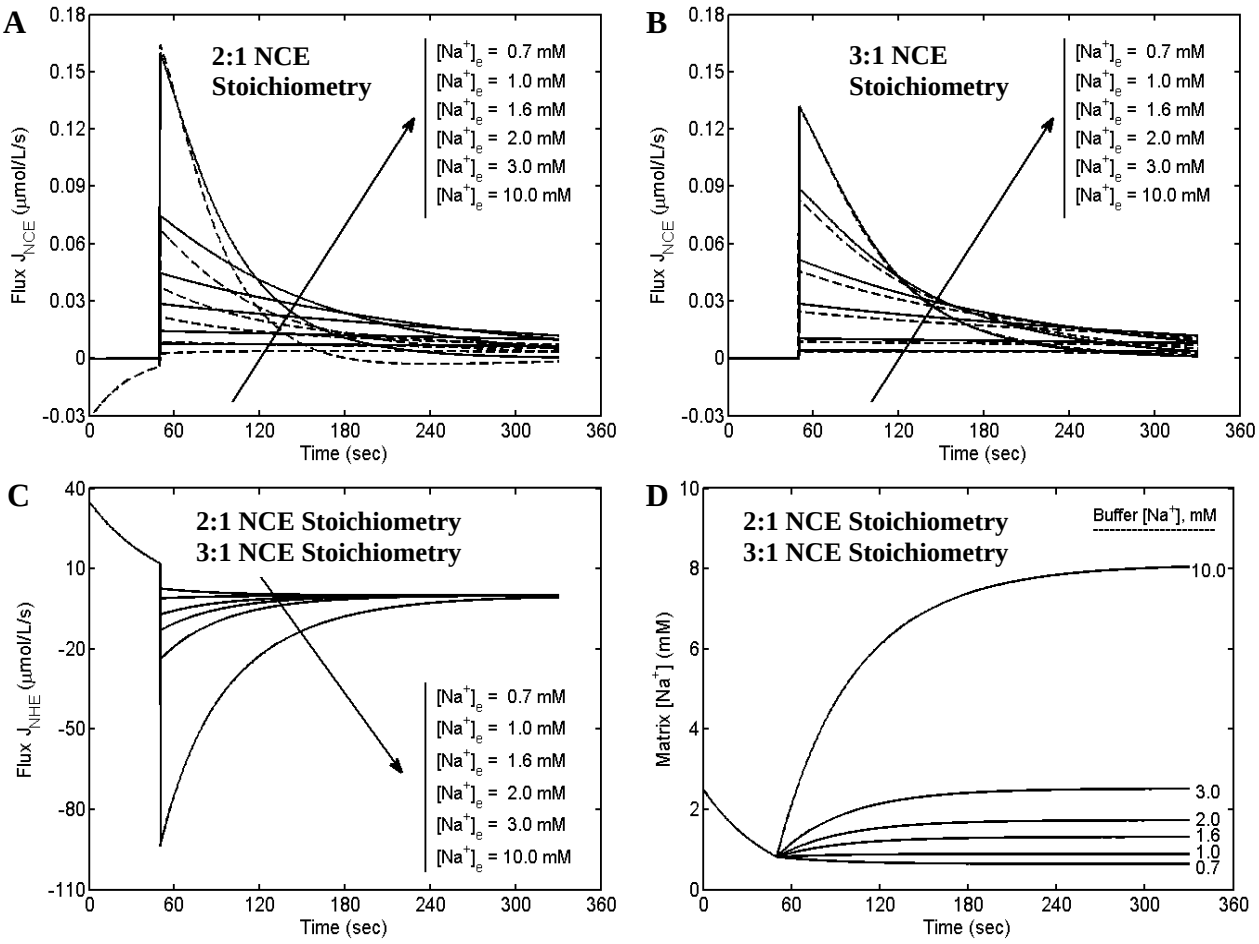

Figure S1. Dynamics of trans-matrix Na^+ fluxes and intra-matrix Na^+ concentrations. (A,B) The model-simulated time courses of Na^+ influx (Ca^{2+} efflux) through the Na^+/Ca^{2+} exchanger (NCE) with the addition of varying levels of Na^+ to the external buffer medium. The model simulation protocol is exactly the same as the experimental protocol of Cox and Matlib (1993) and the model parameter values are exactly the same as those described in Figure 5. The simulations in plot-A are based on using a $2Na^+/Ca^{2+}$ stoichiometry model (electroneutral exchange), while the simulations in plot-B are based on using a $3Na^+/Ca^{2+}$ stoichiometry model (electrogenic exchange). The solid lines are the simulations with a total of 1 μM of Ca^{2+} in the external buffer, while the dashed lines are the simulations with a total of 40 μM of Ca^{2+} in the external buffer. The corresponding model-simulated time courses of Na^+ fluxes through the Na^+/H^+ exchanger (NHE) and the resulting time courses of intra-matrix $[Na^+]$ are shown in plots C and D, respectively. In contrast to the NCE fluxes, both the NHE fluxes and matrix $[Na^+]$ are independent of the external buffer $[Ca^{2+}]$ as well as the NCE stoichiometry.

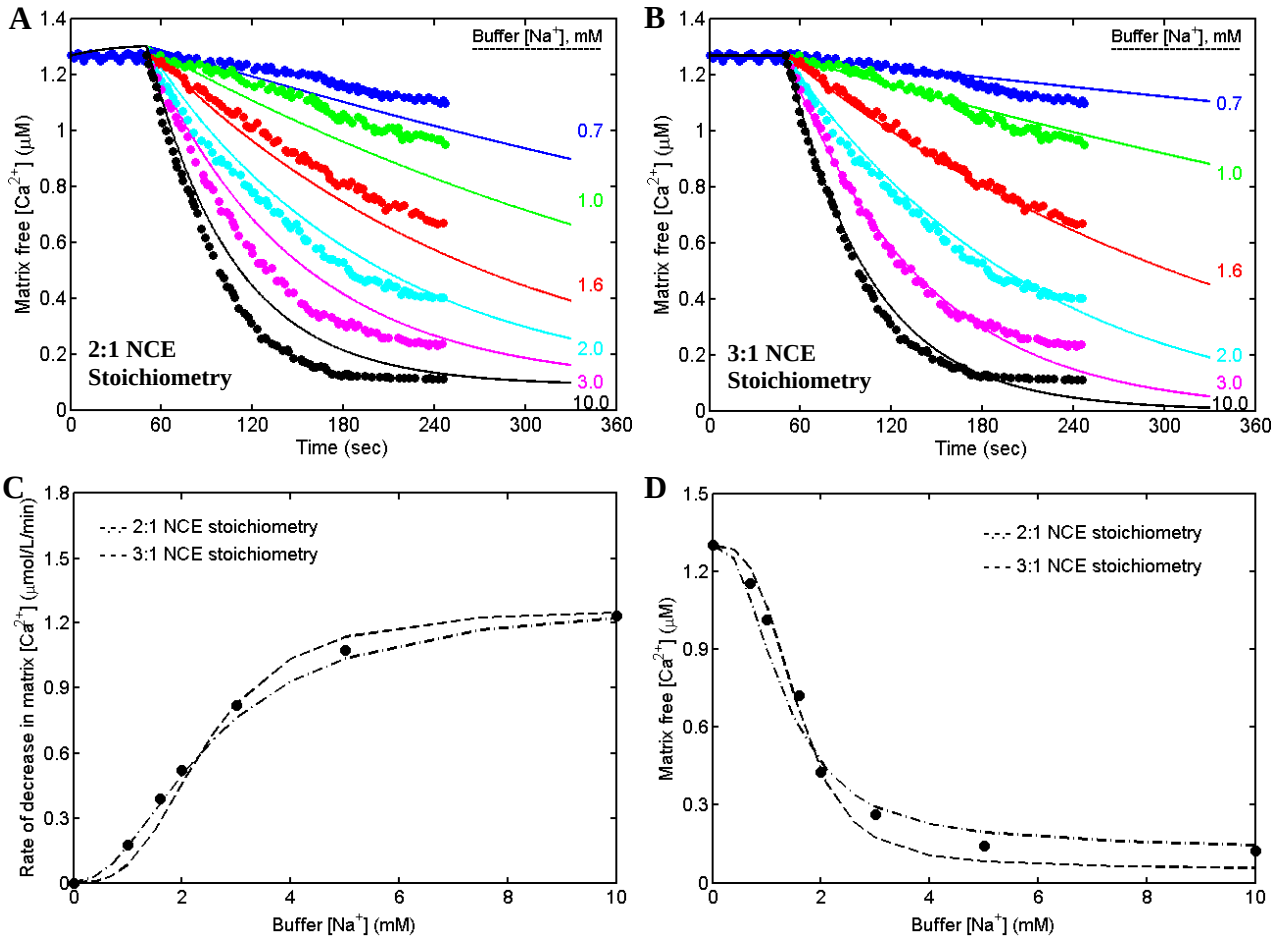

Figure S2. Characterization of the kinetics and stoichiometry of the mitochondrial NCE. The comparison of model predictions (lines) to the experimental data (points) of Cox and Matlib (1993) using both the 2:1 and 3:1 NCE stoichiometry models with the total external buffer $[Ca^{2+}]$ fixed at 20 μM and the NCE model parameter values obtained by fitting the NCE flux expressions (2a) and (2b) to the experimental data on initial NCE flux rates in plot-C. The experimental protocol and data are described in Figure 5. The estimate of ~20 μM of total external buffer $[Ca^{2+}]$ is based on the EGTA-Ca^{2+} binding model (Eq. 5) with a free external buffer $[Ca^{2+}]$ of ~0.15 μM; 0.15 μM is the approximate free external buffer $[Ca^{2+}]$ at steady state with a free matrix $[Ca^{2+}]$ of 0.1 μM (as depicted in the experimental data of Cox and Matlib; plots-A,B) calculated using the 2:1 NCE stoichiometry model with the CU blocked. The NCE model parameter values obtained from the initial NCE flux rate measurements in plot-C are $K_{Na,NCE}$ = 2.4 mM, $K_{Ca,NCE}$ = 2.1 μM, and X_{NCE} = 1.32×10^{-3} nmol Ca^{2+}/mg/s (2.64×10^{-3} nmol Na^{+}/mg/s) for the 2:1 model and $K_{Na,NCE}$ = 2.4 mM, $K_{Ca,NCE}$ = 2.1 μM, and X_{NCE} = 3.375×10^{-5} nmol Ca^{2+}/mg/s (10.125×10^{-5} nmol Na^{+}/mg/s) for the 3:1 model. Note that the NCE model parameter estimates are the same as those in Figure 5 for the 3:1 model, while the estimates of both $K_{Na,NCE}$ and X_{NCE} are reduced for the 2:1 model. Furthermore, the simulations using the $2Na^{+}/Ca^{2+}$ stoichiometry model deviates considerably from the dynamic data (plot-A), while the simulations using the $3Na^{+}/Ca^{2+}$ stoichiometry model is more consistent with the dynamic data (plot-B) throughout the measurement period. This analysis further substantiates the hypothesis of 3:1 NCE stoichiometry.

References

Alberty RA. (2003). *Thermodynamics of Biochemical Reactions*. John Wiley & Sons, Hoboken, N.J.

Beard DA. (2005). A Biophysical Model of the Mitochondrial Respiratory System and Oxidative Phosphorylation. *PLoS Comput Biol* **1,** e36.

Beard DA. (2006). Modeling of oxygen transport and cellular energetics explains observations on in vivo cardiac energy metabolism. *PLoS Comput Biol* **2**.

Bose S, French S, Evans FJ, Joubert F & Balaban RS. (2003). Metabolic network control of oxidative phosphorylation: multiple roles of inorganic phosphate. *J Biol Chem* **278,** 39155-39165.

Cox DA & Matlib MA. (1993). A role for the mitochondrial Na^+-Ca^{2+} exchanger in the regulation of oxidative phosphorylation in isolated heart mitochondria. *J Biol Chem* **268,** 938-947.

Gentet LJ, Stuart GJ & Clements JD. (2000). Direct measurement of specific membrane capacitance in neurons. *Biophys J* **79,** 314-320.

Huang M, Camara AK, Stowe DF, Qi F & Beard DA. (2007). Mitochondrial inner membrane electrophysiology assessed by rhodamine-123 transport and fluorescence. *Ann Biomed Eng* **35,** 1276-1285.

Kapus A, Ligeti E & Fonyo A. (1989). Na^+/H^+ exchange in mitochondria as monitored by BCECF fluorescence. *FEBS Lett* **251,** 49-52.

Lee AC, Zizi M & Colombini M. (1994). Beta-NADH decreases the permeability of the mitochondrial outer membrane to ADP by a factor of 6. *J Biol Chem* **269,** 30974-30980.

Munoz DR, de Almeida M, Lopes EA & Iwamura ES. (1999). Potential definition of the time of death from autolytic myocardial cells: a morphometric study. *Forensic Sci Int* **104,** 81-89.

Tomashek JJ & Brusilow WS. (2000). Stoichiometry of Energy Coupling by Proton-Translocating ATPases: A History of Variability. *J Bioenerg Biomembr* **32,** 493-500.

Vendelin M, Kongas O & Saks V. (2000). Regulation of mitochondrial respiration in heart cells analyzed by reaction-diffusion model of energy transfer. *American Journal of Physiology - Cell Physiology* **278,** C747-764.

Vinnakota KC & Bassingthwaighte JB. (2004). Myocardial density and composition: a basis for calculating intracellular metabolite concentrations. *Am J Physiol Heart Circ Physiol* **286,** H1742-1749.

Wu F, Jeneson JA & Beard DA. (2007a). Oxidative ATP synthesis in skeletal muscle is controlled by substrate feedback. *Am J Physiol Cell Physiol* **292,** C115-124.

Wu F, Yang F, Vinnakota KC & Beard DA. (2007b). Computer modeling of mitochondrial tricarboxylic acid cycle, oxidative phosphorylation, metabolite transport, and electrophysiology. *J Biol Chem* **282,** 24525-24537.